

Polarity Reversal of Active Plate Boundary and Elevated Oceanic Upper Mantle beneath the Collision Suture in Central Eastern Taiwan

by K. H. Kim,* J. M. Chiu, J. Pujol, and K.-C. Chen

Abstract The active collision between the Eurasia and Philippine Sea plates in eastern Taiwan has been explored from the recently determined 3D velocity images and relocated hypocenters. A north-northeast–south-southwest-trending high-velocity zone corresponding to the oceanic upper mantle is narrowly defined underneath the collision suture from Hualien to Taitung. This elevated and hot oceanic upper mantle must have played an important role in the tectonic evolution/mountain-building process of the adjacent continental crust. A northwest-dipping seismic zone can be identified in the northern collision zone extending from the surface to ~30 km depth, which can be correlated with the northern Longitudinal Valley Fault (LVF). This zone marks a transitional plate boundary separating the high V_P and high V_P/V_S oceanic crust to the east and the high V_P and V_S upper crust and low V_P and low V_P/V_S mid-to-lower continental crust to the west. A significant amount of plate convergence along the suture has been accommodated by the high-angle thrusting along the northern LVF. In contrast, a southeast-dipping seismic zone can be identified extending from the surface to ~25 km depth near Taitung in the southern collision zone. This zone coincides with a region of high V_P and high V_P/V_S , suggesting that earthquakes occurred within a highly fractured or fluid-rich zone. The reverse polarity of active-plate boundary faults marks two distinguished transition boundaries, one from eastward subduction in southern Taiwan to east–west collision in the southern collision zone corresponding to the early phase of plate collision, and the other from east–west collision to northwest subduction in the northern collision zone corresponding to the advanced phase of plate collision. The central collision zone is creeping and aseismic, which can be attributed to the high heat flow and geothermal activity during an interseismic period since the 1951 Taitung earthquake.

Introduction

Located along the plate boundary between the Eurasia (EUP) and the Philippine Sea (PSP) plates, the island of Taiwan was formed as a consequence of an arc-continent collision. Deformation and seismicity in and around Taiwan are very active because of the high-convergence rate between the two plates (Yu *et al.*, 1997). The PSP is subducting beneath the EUP in northeastern Taiwan along the Ryukyu trench, while the South China Sea plate, a subplate of the EUP, is subducting beneath the PSP in southern Taiwan along the Manila trench. Active collision is taking place between the two subduction systems in central eastern Taiwan. The Longitudinal Valley (LV), sandwiched between the Central Range (CR) of the EUP and the Coastal Range (COR) of the PSP, is considered as the collision suture between the two

plates (Ho, 1999; Tsai, 1986). The LV is about 160 km long and less than 10 km wide in most places and is filled with Quaternary sediments. The LV is bounded by two north-northeast–south-southwest-trending faults running parallel to each other from Hualien in the north to Taitung in the south. These two bounding faults can be roughly delineated from the topography (Fig. 1), although their surface exposures are rarely seen because of the high-erosion rate and thick sediment cover. Because the PSP converges obliquely toward the EUP, the collision in the northern LV near Hualien is far more advanced than that at the southern LV near Taitung where the collision is in its early stage. The eastern boundary of the LV, the Longitudinal Valley fault (LVF), is a very active high-angle oblique thrust fault with a minor left-lateral strike-slip component (Barrier and Angelier, 1986; Yu *et al.*, 1990; Yu and Kuo, 2001; Yu and Liu, 1989). The LVF can be subdivided into several smaller fault segments including, from north to south, the Luehmei fault

*Present address: Korean Ocean Research and Development Institute, P.O. Box 29, Seoul, 425-600 Korea.

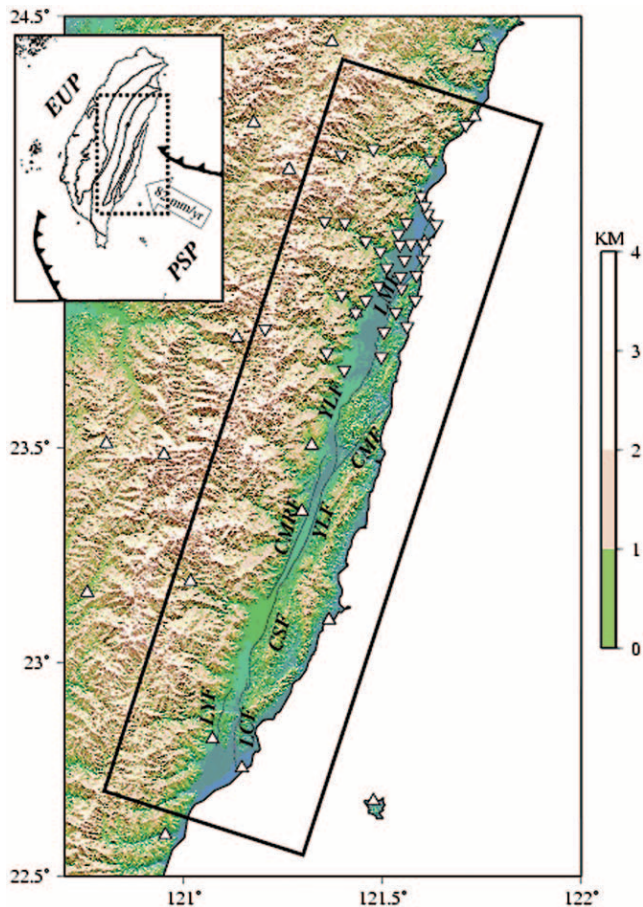


Figure 1. Topography map of the collision zone in central eastern Taiwan showing the collision zone suture (the Longitudinal Valley, LV), oceanic frontal arc (the Coastal Range, COR), and the uplifted continental crust (the Central Range, CR). Collision between the Eurasia plate (EUP) and the Philippine Sea plate (PSP) takes place along the LV with a highly convergent rate at 82 mm/yr (Yu and Liu, 1989; Yu *et al.*, 1990; Yu and Kuo 2001). Boundaries of the major geologic units in the Taiwan area are shown in the index map (upper left) where the dotted box marks the area of the larger map. Seismic stations used in the tomographic inversion are shown by triangles (CWB-TSN) and inverted triangles (PANDA II). Known active faults in the LV and COR (Ho, 1999) are drawn using solid lines including: LMF, Luehmei fault; YUF, Yuli fault; CSF, Chihshang fault; LYF, Luehmei fault; LCF, Lichi fault; CRF, Central Range fault; and CMF, Chimei fault. The study region is outlined by the thick-lined box. Different segments of the LVF have different local names, including the LMF, YLF, CSF, and LCF.

(LMF), the Yuli fault (YLF), the Chihshang fault (CSF), and the Lichi fault (LCF). Moderate to large earthquakes occur frequently along various fault segments in central eastern Taiwan. Earthquakes along the collision zone, however, are not evenly distributed, revealing that the deformation and active faulting associated with the plate collision may vary significantly along different segments of the LVF. For ex-

ample, the central LV and COR, from the Chimei fault to the north of Chengkung, was aseismic in the past 30 years in contrast to the very active southern and northern collision zones. Detailed geodetic and Global Positioning System (GPS) surveys reveal that a significant amount of aseismic deformation, for example, creeping, is taking place along the 50-km-long central segment of the LVF (Yu and Liu, 1989).

Seismicity and its tectonic implications have long been a primary research focus in the eastern Taiwan region. However, the lack of high-resolution local seismic data and the lack of reliable 3D V_p and V_s models have prevented any major improvement in our understanding of where and how earthquakes occur and their correlations with the collision tectonics. Using selected local seismic array data, Lin *et al.* (1998) constructed probably the first comprehensive 3D V_p and V_s models beneath the Hualien region in the northern collision zone. Their results reveal a thin nearly vertical low V_p zone extending from the surface to a depth of at least 20 km beneath the eastern LV and an upward "bulge" of higher velocities beneath the eastern CR. However, because less than 10% of local array data were used in Lin *et al.* (1998), their spatial resolution of structures and accuracy of the relocated seismicity are somewhat restricted in the upper crust within a small region where the local array was deployed (Yeh *et al.*, 1997). Recently, Hao *et al.* (2004) relocated eastern Taiwan earthquakes using the hypo-DD method (Waldhauser and Ellsworth, 2000) and determined focal mechanisms of selected earthquakes to interpret the regional tectonics associated with plate collision. Based on the relocated seismicity, Hao *et al.* (2004) concluded that the LV is an east-dipping suture zone, that both the northern and southern collision zones are characterized by east-dipping seismic zones, and that the EUP subducts to the east under the PSP. Their interpretations are, however, controversial according to some recent observations (e.g., Kim *et al.*, 2005), mainly because of the oversimplified earth model and the uncertainties on Hypo-DD locations for earthquakes mostly outside or at the outer boundary of an islandwide seismic network over very complicated 3D velocity structures.

The seismogenic structures associated with crustal deformation beneath the collision zone in the central-eastern Taiwan can be explored via high-resolution 3D V_p and V_s images (Kim, 2003; Kim *et al.*, 2005) and well-located local earthquakes using the resultant 3D models (Chiu *et al.*, 2003; Chen *et al.*, 2006). In addition to extensive surface geological information and GPS observations, the spatial correlation of seismicity with known active faults and with previously unknown active faults will provide an unprecedented opportunity for us to understand the current status of plate collision and how the plates interact and deform along an active collision boundary.

Data and Method

Two sets of high-quality earthquake data recorded by a large number of permanent and temporary seismic stations

in Taiwan have been selected to determine 3D velocity models and to relocate earthquakes in the central eastern Taiwan region. These data were recorded by the islandwide Taiwan Seismic Network (TSN) and the Portable Array for Numerical Data Acquisition II (PANDA II) deployed in the Hualien area (Fig. 2). The TSN is operated by the Central Weather Bureau (CWB) and consists of 78 three-component short-period stations. All the arrival times and earthquake-location files from 1991 to 2002 reported by the CWB have been collected and analyzed in this study. The events selected for velocity determination must have been reported by more than 10 high-quality P arrivals (uncertainties less than 0.1 sec) and by more than five high-quality S arrivals (uncertainties less than 0.2 sec). Event-station pairs with an epicentral distance greater than 140 km are excluded for a better approximation to a flat earth (Snoke and Lahr, 2001). In total, 6285 events with 69,758 P -wave arrival times and 42,733 S -wave arrival times were selected from the CWB earthquake catalog for the entire Taiwan region. Between 1993 and 1995, a PANDA II seismic array with 30 three-component short-period seismic stations was deployed in the Hualien area for 30 months by the Institute of Earth Science, Academia Sinica, and the Center for Earthquake Research and Information, the University of Memphis, to study the complex transitional structure associated with the collision tectonics along the northern suture zone between the EUP and the PSP (Chen, 1995; Yeh *et al.*, 1997). Some stations were relocated during the deployment, so that the number of sites occupied by the PANDA II stations is 35. From the best selected 1218 local events, 17,461 P -wave arrivals and 10,003 S -wave arrivals are included in this study.

The 3D tomographic inversion package developed by Benz *et al.* (1996) and modified by Shen (1999) was used to determine 3D V_P and V_S models beneath the collision zone in central eastern Taiwan. A robust finite-difference method based on Huygens' principle proposed by Povdin and Lecomte (1991) is been applied for travel-time calculation. This method has been demonstrated to be very efficient and accurate when complex velocity structures are involved (Benz *et al.*, 1996; Okubo *et al.*, 1997; Villasenor *et al.*, 1998). Thus, this inversion package is suitable to deal with the complex tectonic environment beneath the collision zone in the central eastern Taiwan region.

The velocity structure for the entire Taiwan region has been parameterized by a 3D grid model covering 256 km in the east–west direction, 416 km in the north–south direction, and 152 km in depth with 4 km above and 148 km below the sea level (Fig. 2). The grid size is $8 \times 8 \times 2$ km for velocity inversion and $2 \times 2 \times 2$ km, for travel-time calculation. A smaller block size is adopted for travel-time calculation to ensure a smoother traveling path for travel-time calculation than that with a larger block size. The coordinates are given in kilometers east and north of a reference point at 119.8° E and 21.6° N. Depth is referenced to sea level.

From a Joint Hypocenter Determination (JHD) analysis

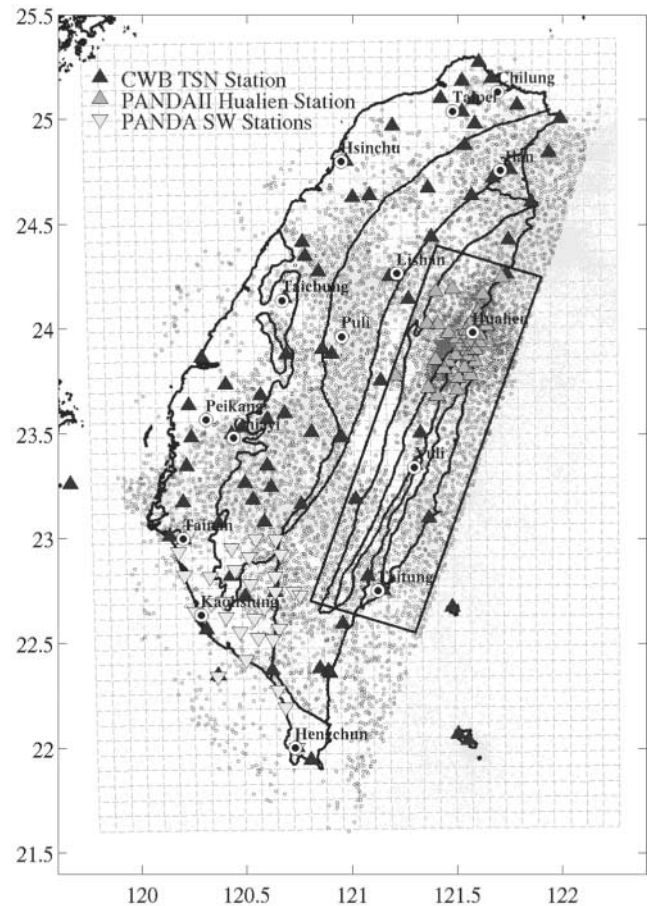


Figure 2. Seismic stations used for islandwide seismic tomography, including CWB-TSN stations (filled triangles), PANDA II–Hualien stations (gray triangles), and PANDA–Pingtung stations (inverted open triangles). Small open circles are the selected earthquake locations from the CWB catalog for the 3D tomographic study. A map view of the 3D velocity grids with 8 km length in the east–west and north–south directions is shown (dashed lines). The study area in central eastern Taiwan is marked by the rectangular box.

of a few selected earthquake clusters, Kim *et al.* (2005) concluded that the uppermost few kilometers of the crust in the Taiwan region is responsible for very significant P - and S -station travel-time residuals. For example, the P -wave residuals vary from up to +2.0 sec for stations in the sedimentary basins to up to –2.0 sec for stations on the mountains. Hypocenters will be seriously mislocated when a 1D homogeneous velocity model is used. Furthermore, because most selected earthquakes are deeper than 5 km and their seismic ray paths in the uppermost few kilometers of the crust are mostly parallel to each other, spatial resolution of the 3D inversion is poor for the uppermost blocks. Thus, an optimum initial velocity model, especially for the uppermost blocks, is essential to obtain reliable inversion results (Kissling *et al.*, 1994). Considering station corrections for P and S waves from the JHD analysis, Kim (2003) and Kim *et al.*

(2005) were able to design optimal initial V_P and V_S models to determine 3D models for the entire Taiwan region. The resultant 3D V_P and V_S models were further validated by a comparison of the observed and synthetic JHD station corrections for P and S waves (Kim 2003; Kim *et al.*, 2005). Large-scale 3D structural models beneath the collision zone were presented in Kim (2003) and Kim *et al.* (2005). However, local structural images and relocated seismicity patterns beneath the collision zone are explored in detail in this article.

The earthquakes recorded by the CWB and PANDA II networks were originally located using a 1D homogeneous layered velocity model. JHD analysis of a few randomly selected earthquake clusters in the Taiwan region revealed that the original hypocenters located using the original 1D are systematically shifted toward the region of higher velocity, for example, the CR in the Taiwan region (Kim, 2003). To correlate earthquake activities with the resultant 3D V_P and V_S models, earthquakes in the CWB catalog will have to be relocated by a better model with a better technique. There were, however, only about 10% of earthquakes in the CWB catalog selected for 3D inversion and thus simultaneously relocated. In this study, all earthquakes from the CWB catalog are relocated by applying a newly developed single-event location algorithm using the resultant 3D V_P and V_S models (Chen *et al.*, 2006).

Results and Discussion

Subsurface structures inferred from the resultant 3D V_P and V_S models along with the well-relocated hypocenters provide us an unprecedented opportunity to explore the characteristic structural features and their deformation associated with the tectonic evolution and current state of plate collision. A few thin-sliced horizontal map views of relocated seismicity at various depths along with the associated V_P and V_S perturbations in the background are shown in Figure 3. In general, seismicity associated with the collision zone is oriented parallel to the north-northeast–south-southwest-trending regional structures, particularly clear at a depth 20 km (Fig. 3). Seismicity in the central collision zone is extremely low and is sandwiched between the very active northern and southern collision zones. It is also apparent that seismicity seems to shift from directly beneath the LV at shallow depth (10 km) to outside the LV at deeper depth (e.g., 20 km) in opposite directions for the northern and southern collision zones, respectively. Thus, the current status of plate collision and its associated seismicity seem to be different between the northern and southern collision zones.

Synthetic Tests

A checkerboard resolution test (CRT) (Zhao *et al.*, 1992; Hole *et al.*, 2000) has been applied to explore the ray coverage and spatial resolution of the velocity models in central

eastern Taiwan. The 3D P - and S -wave checkerboard velocity models were constructed by adding $\pm 5\%$ of sinusoidal velocity variations to the initial 1D homogeneous layered model. Results of the CRT are presented in map views at different depths (Fig. 4). In general, the checkerboard patterns in the northern LV and COR have been resolved better than those in the south mainly because of the availability of the PANDA II seismic data in the Hualien region (Yeh *et al.*, 1997). Checkerboard patterns beneath the offshore area are not well recovered because earthquakes outside of the coverage area of the seismic network are excluded to prevent any uncertainties posed by poor azimuthal coverage and poor location. Overall, the original checkerboard velocity patterns for P and S waves beneath the collision zone in the central eastern Taiwan can be successfully recovered at least to a depth of 30 km. The CRT confirms that seismogenic structures associated with the active plate collision in the central eastern Taiwan can be successfully retrieved from the existing seismic stations–earthquakes configuration in the Taiwan region. Two other synthetic tests were also performed to evaluate the effect of noises in the arrival time data (e.g., picking errors) and to validate the resultant 3D models. Details of these two tests were reported in Kim *et al.* (2005) and are not repeated here.

The Northern Collision Zone

The resultant 3D V_P and V_S models beneath the LV and COR near the Hualien region in the northern collision zone show significant lateral and vertical variations (Fig. 5). From the cross section EE' and the others to the north, a cluster of northwest-dipping planar seismicity extending from the surface to a depth ~ 30 km can be identified (Fig. 5). Although the planar feature of this northwest-dipping seismicity is best seen as a continuous feature on DD', seismicity in other cross sections to the north of EE' can be projected into the same dipping zone. The surface exposure of this northwest-dipping seismic zone coincides with the northern LVF, that is, the LMF (Fig. 1). Furthermore, the steeply northwest-dipping northern LVF clearly marks the western boundary of a narrowly confined and anomalously elevated high-velocity zone that can be observed consistently beneath the collision suture zone. The western boundary and shallow portions of the eastern boundary (at least to a depth of ~ 20 km) of this high-velocity zone are well constrained inside the islandwide seismic network (Fig. 4). This high-velocity zone is elongated following the orientation of the north-northeast–south-southwest-trending LV and seems to have a deep origin associated with the oceanic upper mantle. The uppermost region of this zone reaches to ~ 15 km depth with velocity ≥ 7.0 km/sec that can only be found in the lower crust at depths > 30 km beneath the adjacent CR. Thus, the crust beneath the northern collision zone suture is relatively thin in comparison with that beneath the CR. The steeply dipping LVF is sandwiched between a region of low V_P/V_S to the northwest and a region

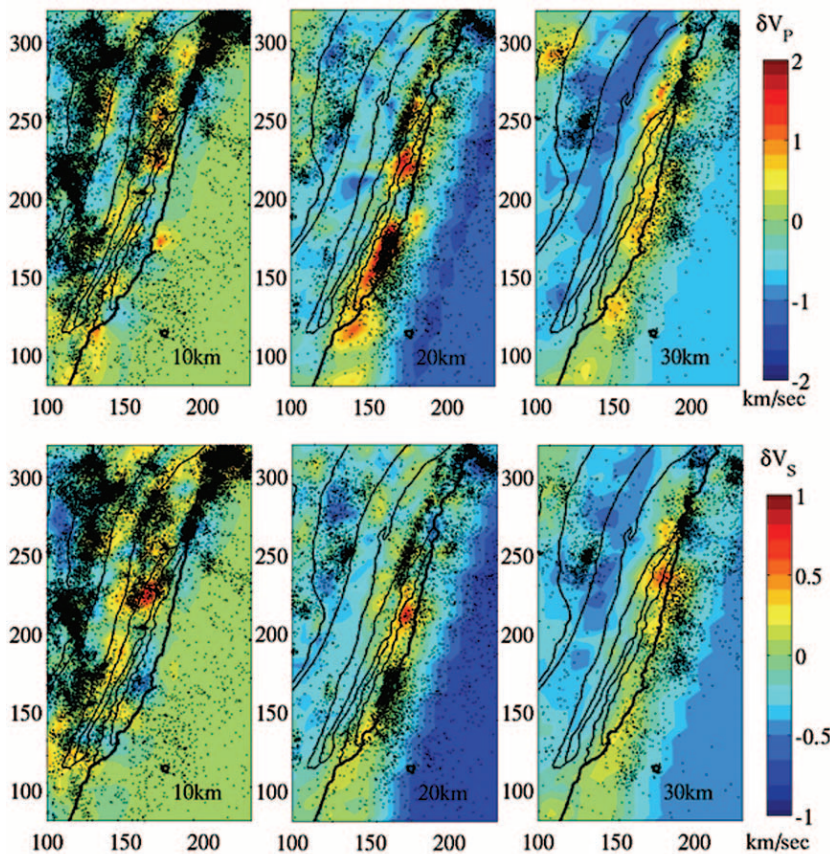


Figure 3. Map views of seismicity and horizontal slices of P - (top) and S -wave velocity anomalies (bottom) at selected depths (shown in the lower-right corner). Regions of significant high-velocity anomaly are observed beneath the collision suture zone. All earthquakes in the CWB catalog between 1991 and 2002 are relocated by a newly developed location algorithm (Chen *et al.*, 2006) using the resultant 3D V_p and V_s models. The relocated seismicity and velocity anomalies are distributed along the north-northwest–south-southwest orientation of the major geologic divisions on the surface.

of high V_p/V_s to the southeast (Fig. 6). V_p and V_p/V_s are expected to increase if rock composition changes from felsic to mafic, or if rocks have more Fe or Mg contents (Fowler, 1990). Conversely, V_p/V_s will decrease with an increase in silica content, as in the continental crust (Christensen, 1996). Thus, the seismically active LVF in the northern collision zone marks a plate boundary between the silica-rich continental crust to the northwest and the Mg- and Fe-rich oceanic crust to the southeast.

Using GPS data, Yu *et al.* (1997) and Yu and Kuo (2001) reported that the convergence velocity between the EUP and PSP plates is consistently about 56–70 mm/yr along most of the LV. The plate-convergence velocity is, however, reduced dramatically to 11–40 mm/yr near the Fengping area in the northern LV, corresponding to the area near EE' in Figure 5. The sudden reduction of convergence velocity north of EE' reveals that a significant amount of plate convergence may have been accommodated along the steeply northwest-dipping northern LVF, that is, the LMF, forming a transition region from the active collision to the active subduction further to the north.

The Central Collision Zone

One of the most noticeable observations in the central collision zone is its relatively low seismicity, in contrast to the very active southern and northern segments (Fig. 7). This

low-seismicity region has long been recognized for its creeping activity (Yu and Liu, 1989; Yu *et al.*, 1990; Yu and Kuo, 2001) and for its high surface heat flow and hot springs (Lee and Cheng, 1986; Wang *et al.*, 1994). Wang *et al.* (1994) suggested that high geothermal activity is one of the most important factors associated with the zones of low seismicity observed in the CR and the central LV. Heat sources in the region may be supplied by the hot oceanic upper mantle beneath the thin crust of the collision suture. The oceanic upper mantle is expected to be hotter than the adjacent mid-continental crust at the same depth. The mid to lower crust of the adjacent continent and the crust of the collision suture above is expected to receive excess heat from the elevated oceanic upper mantle. In addition, shear heating from the active collision boundary may also supply extra heat sources for the creeping deformation (Ma *et al.*, 1996). The excessive heat supply in the central LV may contribute in part to the creeping and low seismicity in the central LV region.

In addition, the central collision zone is also the region of a few large historical earthquakes (Fig. 7). Among them, the 1951 Taitung earthquake (M_L 7.3), the second largest inland earthquake, occurred in Taiwan during the twentieth century (Cheng *et al.*, 1996, 1999). The mainshock was followed immediately by two large aftershocks (M_L 7.1) and many smaller aftershocks that ruptured the CSF and the YLF (Cheng *et al.*, 1996, 1999). Since the 1951 earthquake sequence, the entire 50-km span of the central LV, approxi-

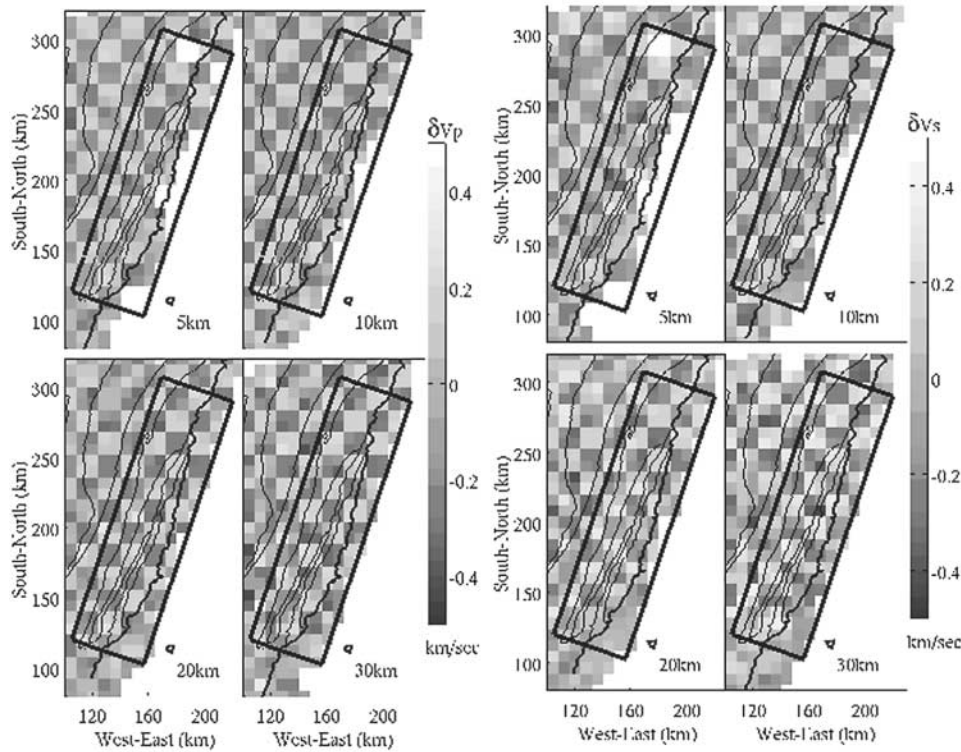


Figure 4. Map views of the reconstructed checkerboard velocity patterns for P (left) and S waves (right) at various depths (shown in the lower-right corner). The study area is marked by the rectangular box. The original checkerboard velocity patterns can be successfully retrieved at least to 30 km depth for both P and S waves.

mately corresponding to the Yuli fault, is basically aseismic. Based on the recent geodetic surveys and GPS observations, the central segment of the LV is undergoing significant creeping with both vertical and horizontal motions (Yu and Liu, 1989; Yu *et al.*, 1997; Yu and Kuo, 2001). Thus, the lack of seismicity in the central collision zone during the past 30 years may also be because the region is experiencing an interseismic period between large earthquakes.

The Southern Collision Zone

Beneath the southern collision zone, a layer of low-velocity materials was imaged in the uppermost crust, whose thickness gradually increases toward the east (Fig. 8). Materials within this low-velocity layer may be associated with large amounts of sediment eroded and transported from the high CR and COR into the lower LV or into the ocean. Similar to the observations in the northern collision zone, a narrowly confined, anomalously elevated, and north-south elongated high-velocity zone is consistently imaged beneath the southern collision suture. The uppermost depth of this high-velocity zone is about 12 to 14 km, slightly shallower than that in the northern collision zone. This elevated oceanic upper mantle is consistently observed beneath the entire collision suture from Hualien in the north to Taitung in the south. From a few shallow earthquakes that occurred in the northern LV, Liang and Chiu (2006) reported that anomalous

Pn waves were observed at stations along the LV at epicenter distances as short as 60 km. They concluded that the crust beneath the LV must be extremely thin compared with the adjacent CR, that is, the observed oceanic upper mantle must be significantly elevated and the Moho depth must be very shallow beneath the LV in central eastern Taiwan. The elevated oceanic upper mantle is bounded in the west by an active vertical fault, the Luyeh fault (LYF), and in the east by a very active eastward-dipping fault extending from near the surface in the western COR to a depth of ~ 25 km offshore. The LYF may be longer than previously known (Ho, 1999) and may have extended northward to join the CRF. The most concentrated east-dipping seismicity occurs at depths between 10 and 20 km beneath the Coastal Range (Fig. 8; BB' and CC'). This east-dipping seismic zone coincides with regions of high V_p/V_s ratio (Fig. 9), which may imply the existence of fluid or a highly fractured zone due to the collision. This active seismic zone is thus most probably the plate boundary fault separating the continental crust to the west across the suture zone and the oceanic crust to the east. The corresponding fault on the surface for this east-dipping seismic zone is probably located to the east of the CSF in western COR, which requires further validation. Most recently, the December 2003 M_L 6.6 Chengkung earthquake and its aftershock sequence occurred along this east-dipping plate boundary fault (Chen, 2004). Recent studies of strong

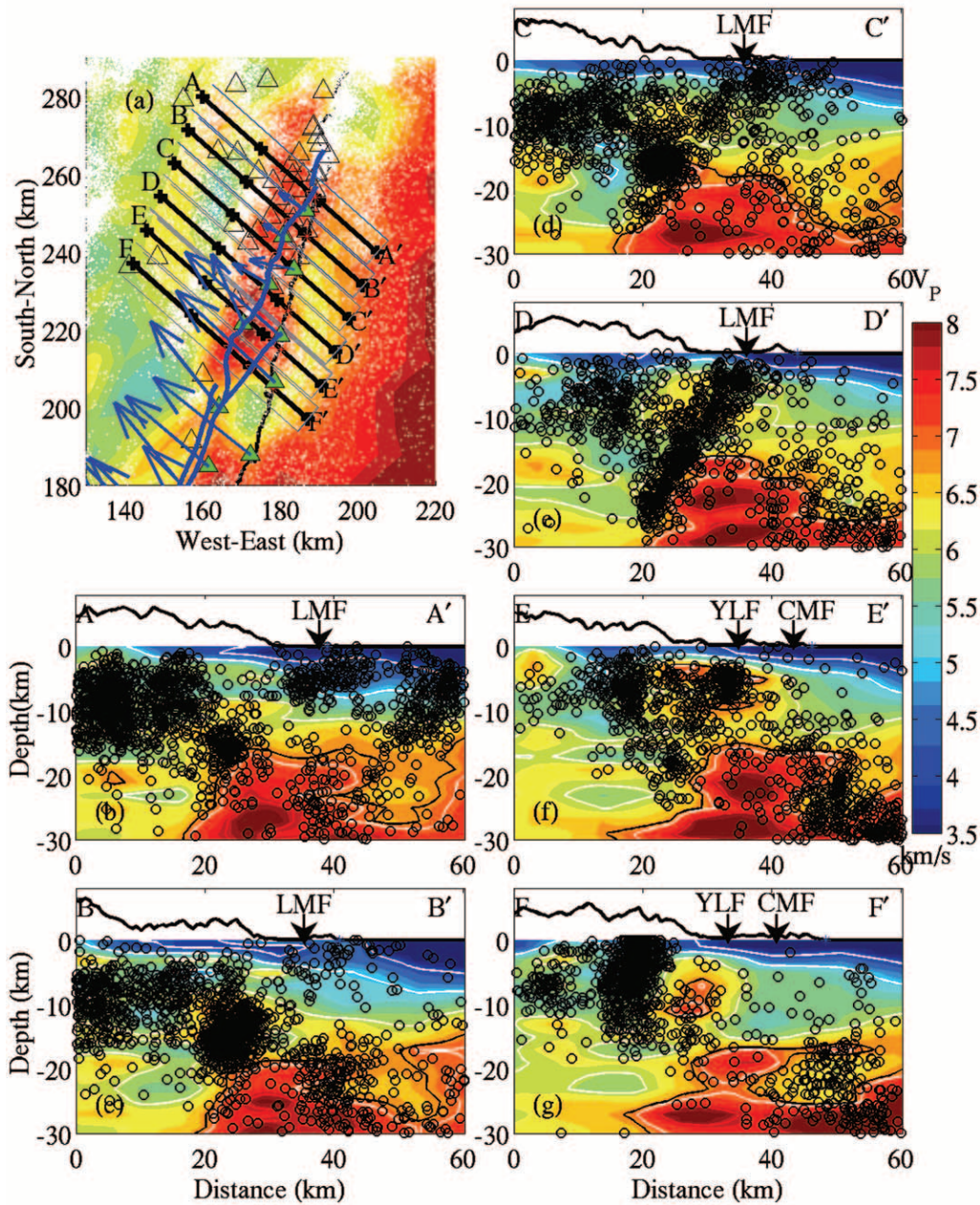


Figure 5. Index map (upper left) and six cross-sectional views of relocated seismicity in the northern LV with the resultant V_p from the inversion in the background. V_p at 20 km is plotted in the map view, where open triangles are seismic stations, green triangles are GPS stations, blue arrows mark the velocity field of the plate convergence reported from the GPS study of Yu *et al.* (1997), blue lines are the map view of active faults, and white dots are earthquakes within ± 3 km from the selected depth. Surface elevation on top of each cross section is vertically exaggerated ($\times 2$). Surface locations of the northern LVF (LMF and YLF) are marked by the arrows.

ground motion and coseismic GPS observation suggest that the 2003 Chengkung earthquake sequence along this east-dipping fault is most probably related to the CSF. Hao *et al.* (2004) relocated earthquakes in eastern Taiwan and reported dominantly thrust faulting along this east-dipping fault. Their conclusion that the EUP subducts to the east underneath the PSP in the southern collision zone may make sense

based only on the spatial distribution of their relocated seismicity. However, the observations of the elevated and north-south-elongated oceanic upper mantle to the west behind the east-dipping plate boundary fault (Figs. 8 and 9) may reveal other interpretations. Because the collision in the southern zone is most probably in its early stage, earthquakes occur mainly along the collision boundary characterized by a

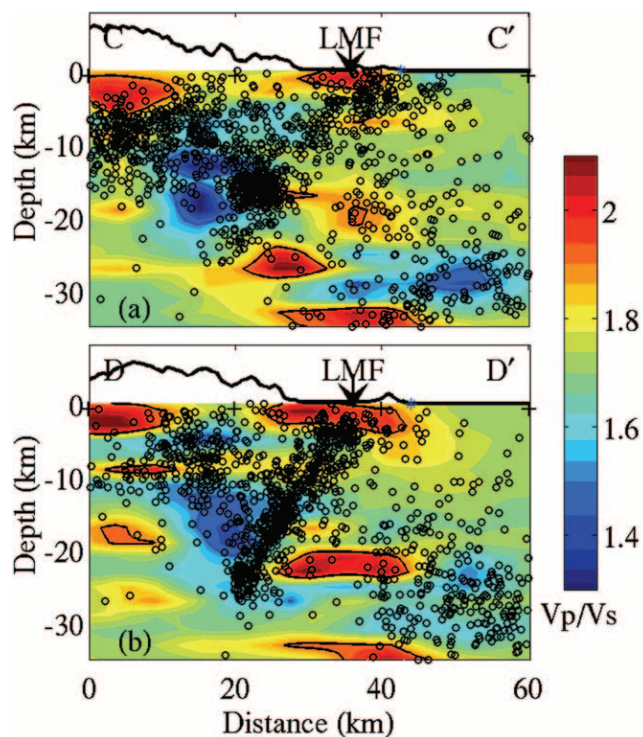


Figure 6. Two cross-sectional views of the seismicity along CC' and DD' in Figure 5. V_p/V_s information is plotted in the background. Surface elevation shown on top of each cross section is vertically exaggerated ($\times 2$). Location of the northern LVF (the LMF) is also marked.

highly fractured zone with a high V_p/V_s ratio. Water content inside this collision zone may play a very important role in the excitation of earthquakes.

Seismicity and Active Faults

Many active faults in central eastern Taiwan (Fig. 1) are mapped basically from surface geology and seismicity (e.g., Ho, 1999; Lee, 1999). These faults are mostly parallel to the north-northeast–south-southwest-trending collision suture. Undoubtedly, the LVF, located at the eastern boundary of the LV, is the most dominant fault in the collision zone. The LVF also has a local name at different segments of the LV, for example, the Luehmei fault (LMF) in the north, the Yuli fault (YLF) in the center with the Chimei fault (CMF) branch out into COR, and the Chihshang fault (CSF) and Lichi fault (LCF) in the south (Fig. 1). Other active faults, for example, the Luyeh fault (LYF) and the Central Range fault (CRF), are shorter and parallel to the LVF. These active faults are closely related to deformation associated with the plate collision. Earthquakes that occur along an active fault or fault segment can be studied to explore the dynamics and tectonics of faulting during collision. Not all of these faults or fault segments are currently seismically active, however (Fig. 3). Reliable earthquake location and high-resolution 3D V_p and V_s structural models are the keys for a successful imaging

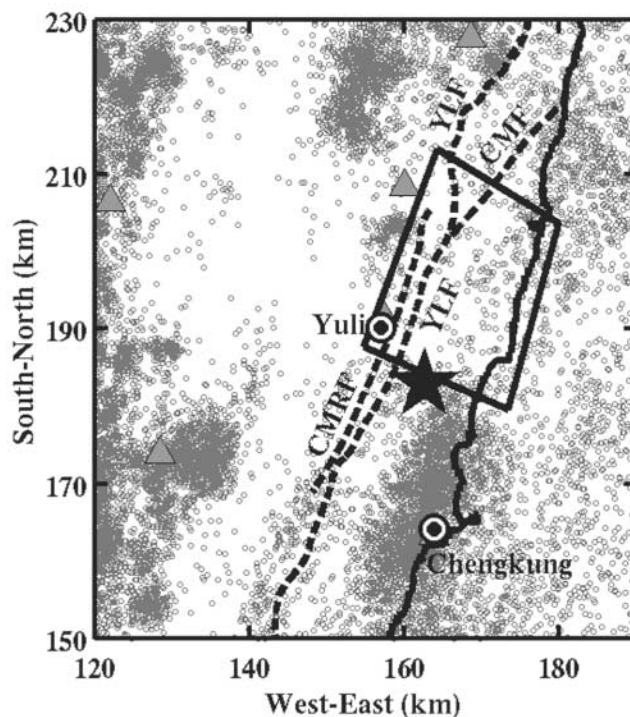


Figure 7. Map showing the background seismicity (small open circles) and known active faults (thick dashed lines) in the central collision zone. Known active fault locations are from Lee (1999) and Ho (1999). Location of the 1951 Taitung earthquake is marked by the filled star (Cheng *et al.*, 1996, 1999). Solid grey triangles are the locations of CWB seismic stations. Seismicity in the central collision zone is relatively low in comparison with that in the northern and southern collision zones.

of the geometry of the faults to improve our understanding of the roles of each fault in the collision tectonics. In addition to the major active faults discussed earlier, the vertical seismicity clearly identified in CC', DD', and EE' of Figure 8 can be associated with the LYF, suggesting that the LYF is probably longer than previously reported from surface geology alone (Ho, 1999; Lee, 1999). The LYF may extend north to connect to the CRF, so that potential for a large earthquake cannot be overlooked. An apparently aseismic region can be clearly identified separating the LYF and a cluster of upper-crust seismicity in the CR (CC', DD', and EE', Figure 8). The sharp seismicity boundary in the eastern CR to the west of the aseismic region may suggest an active fault.

Conclusions

The well-located earthquakes and high-resolution 3D V_p and V_s models presented in this study enable us to explore the complex tectonic structures associated with active plate collision in eastern Taiwan. Crust and upper-mantle structural images beneath the collision suture zone become es-

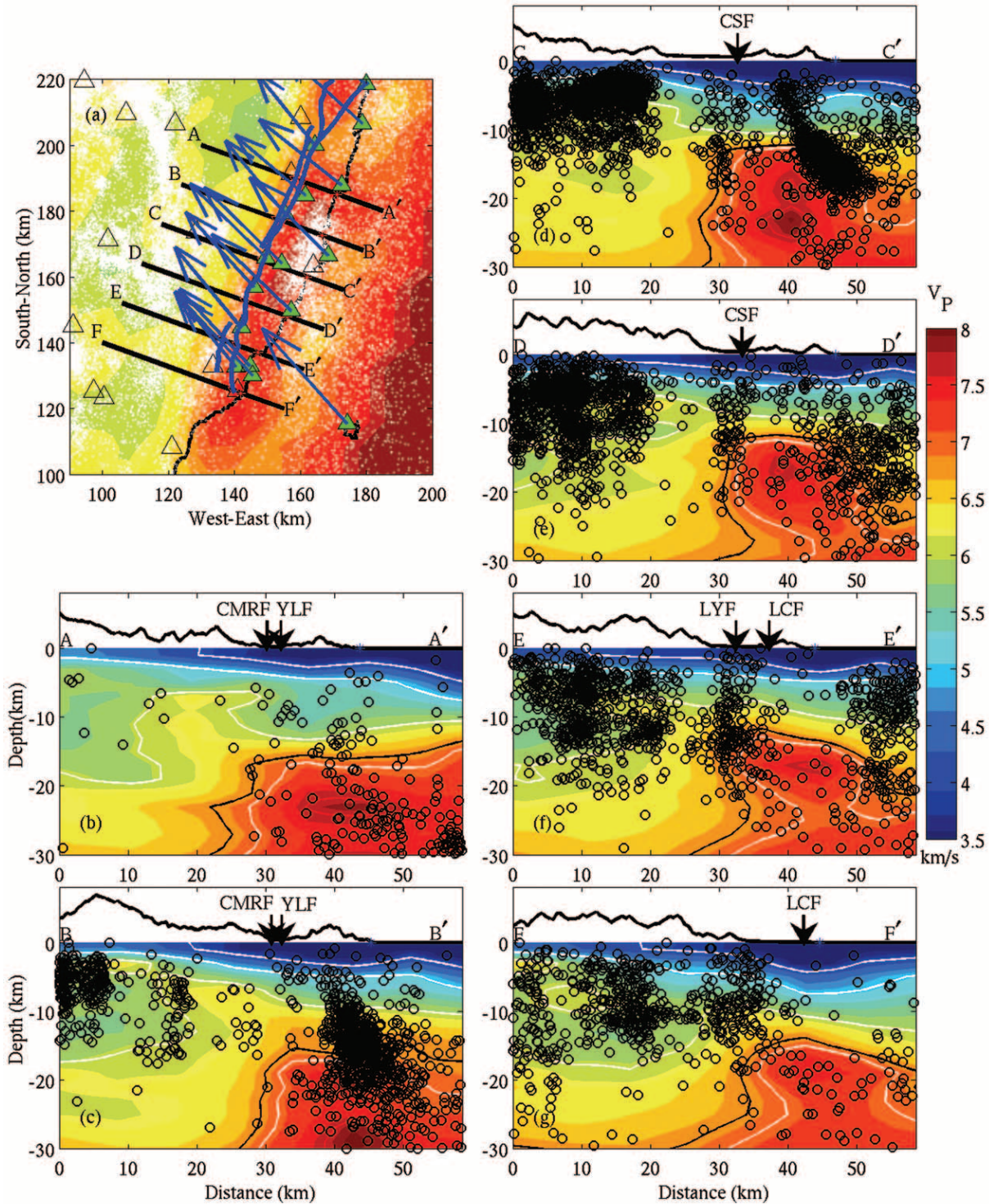


Figure 8. Index map (upper left) and six cross-sectional views of relocated seismicity in the southern LV with the resultant V_p from the inversion in the background. V_p at 20 km is plotted in the map view, where open triangles are seismic stations, green triangles are GPS stations, blue arrows mark the velocity field of the plate convergence reported from the GPS study of Yu *et al.* (1997), blue lines are the map view of active faults, and white dots are earthquakes within ± 3 km from the selected depth. Surface elevation on top of each cross section is vertically exaggerated ($\times 2$). Surface locations of the southern LVF (YLF, CSF, and LCF) and two other shorter faults (CRF and LYF) are marked by the arrows.

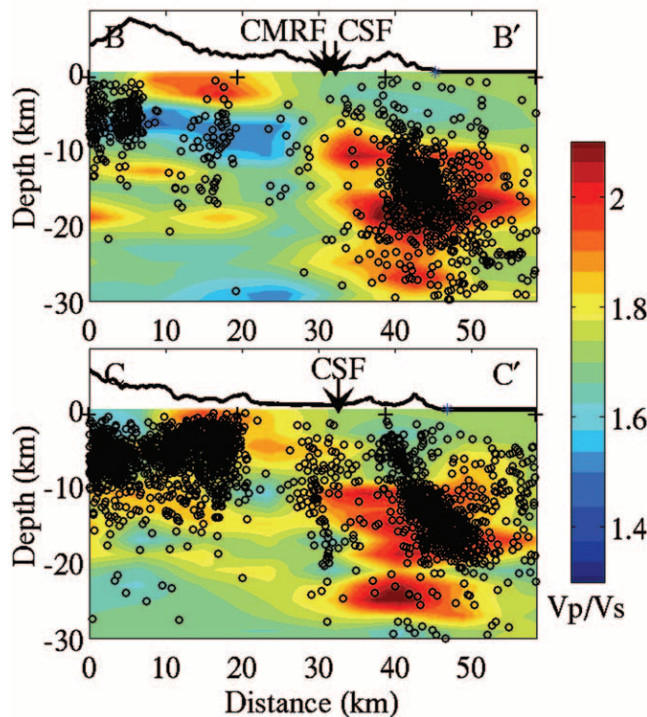


Figure 9. Two cross-sectional views of the seismicity along BB' and CC' in Figure 8. V_p/V_s information is plotted in the background. Surface elevation shown on top of each cross section is vertically exaggerated ($\times 2$). Surface locations of the southern LVF (CSF) and one adjacent shorter fault (CRF) are also marked.

essential to our understanding of the regional tectonics evolution. A narrowly confined, anomalously elevated, and north-northwest–south-southwest-elongated oceanic upper mantle can be clearly identified beneath the Longitudinal Valley from Hualien in the north to Taitung in the south. The existence of this hot oceanic upper mantle beneath the entire collision suture zone, that is, the LV, suggests that heat sources and geothermal activities may play very important roles in the evolution of the collision tectonics in eastern Taiwan, which is the key to the tectonic evolution of the entire Taiwan region. In addition to the main plate boundary fault, that is, the LVF, the well-located hypocenters allow the identification of a few shorter active faults, some previously known and a few previously unknown. These faults are mostly parallel to the LVF and represent the secondary deformation of the plates due to collision. The steeply north-west-dipping collision plate boundary in the northern LVF seems to correlate well with a sudden decrease of the high-convergence velocity between the EUP and PSP. Therefore, a large amount of plate convergence in eastern Taiwan must have been accommodated along the LVF in the northern collision zone. This northwest-dipping boundary fault is also consistent with the orientation of the northwest subduction of the PSP underneath the EUP further to the north in north-eastern Taiwan. Thus, the northern collision zone marks the

transition region from plate collision to plate subduction further to the north. In contrast, the steeply southeast-dipping plate boundary in the southern LVF seems to correlate well with a zone of high V_p/V_s corresponding to a highly fractured region associated with the early state of plate collision. This east-dipping plate boundary fault is consistent with the orientation of eastward subduction of the South China Sea subplate underneath the PSP further to the south. Therefore, the southern collision zone marks the transition region from eastward subduction into plate collision. Significant creeping and high geothermal activities have been reported in the central collision zone, indicating that the area is very active. The lack of seismicity along the ~ 50 -km-long central collision zone is probably partially because of the high heat flow and high geothermal activities (Lee and Cheng, 1986; Wang *et al.*, 1994; Ma *et al.*, 1996) and mainly because the area has been undergoing an interseismic quiescent period since the 1951 Taitung earthquake (Cheng *et al.*, 1996, 1999).

Acknowledgments

We thank Dr. Harley M. Benz of the U.S. Geological Survey for allowing us to use his 3D tomographic inversion software. This study was sponsored by the Center of Excellence program at CERI, University of Memphis. K.H.K. was supported by a University Academic Excellence program for his postdoctoral research at NCU and by the National Science Council, Taiwan, under Grant NSC93-2119-M-001-016, for his postdoctoral research at the Institute of Earth Sciences, Academia Sinica. Our sincere thanks also go to Dr. Honn Kao of the Canadian Geological Survey and another anonymous reviewer whose critical comments have significantly improved the content of this manuscript. Most figures were generated using the GMT software (Wessel and Smith, 1991, 1995). This study is also funded in part by KORDI grants PM37500, PE97006, and PP06401 (K.H. Kim). This is CERI contribution number 495.

References

- Barrier, E., and J. Angelier (1986). Active collision in eastern Taiwan: the Coastal Range, *Tectonophysics* **125**, no. 1–3, 39–72.
- Benz, H. M., B. A. Chout, P. B. Dawson, J. C. Lahr, R. A. Page, and J. A. Hole (1996). Three-dimensional P and S wave velocity structure of Redoubt Volcano, Alaska, *J. Geophys. Res.* **101**, no. 4, 8111–8128.
- Chen, H., J. M. Chiu, J. Pujol, K. H. Kim, K. C. Chen, B. S. Huang, Y. H. Yeh, and S. C. Chiu (2006). A simple algorithm for local earthquake location using 3-dimensional V_p and V_s models—test examples in the central USA and Taiwan regions, *Bull. Seism. Soc. Am.* **96**, no. 1, 288–305.
- Chen, K. C. (1995). Earthquake studies using the PANDA and PANDA II seismic arrays, *Ph.D. Thesis*, The University of Memphis, Memphis, 120 pp.
- Chen, K. C. (2004). Relocation of the Dec. 10, 2003 Chengkung earthquake sequence, in *Western Pacific Geophysics Meeting (WPGM)*, American Geophysical Union, Hawaii.
- Cheng, S. N., Y. T. Yeh, M. T. Hsu, and T. C. Shin (1999). *Photo Album of Ten Disastrous Earthquakes in Taiwan*, Central Weather Bureau, Taipei, Taiwan, 289 p.
- Cheng, S. N., Y. T. Yeh, and M. S. Yu (1996). The 1951 Taitung earthquake in Taiwan, *J. Geol. Soc. China* **39**, no. 3, 267–285.
- Chiu, J. M., H. Chen, J. Pujol, S. C. Chiu, and M. Withers (2003). A new earthquake catalog for the New Madrid Seismic Zone using a prelim-

- inary 3-dimensional V_p and V_s velocity model, *Seism. Res. Lett.* **74**, no. 1, 69.
- Christensen, N. I. (1996). Poisson's ratio and crustal seismology, *J. Geophys. Res.* **101**, no. B2, 3139–3159.
- Fowler, C. M. R. (1990). *The Solid Earth: An Introduction to Global Geophysics*, Cambridge University Press, New York, 472 pp.
- Hao, K. C., Y. M. Wu, C. H. Chang, J. C. Hu, and W. S. Chen (2004). Relocation of eastern Taiwan earthquakes and tectonic implications, *TAO* **15**, no. 4, 647–666.
- Ho, C. S. (1999). An introduction to the geology of Taiwan explanatory text of the geologic map of Taiwan, *Central Geological Survey/The Ministry of Economic Affairs*.
- Hole, J. A., T. M. Brocher, S. L. Klemperer, T. E. Parsons, H. M. Benz, and K. P. Furlong (2000). Three-dimensional seismic velocity structure of the San Francisco Bay area, *J. Geophys. Res.* **105**, no. 6, 13,859–13,874.
- Kim, K. H. (2003). Subsurface structure, seismicity patterns, and their implication to tectonic evolution in Taiwan, *Ph.D. Thesis*, The University of Memphis, Memphis, 159 pp.
- Kim, K. H., J. M. Chiu, J. Pujol, K. C. Chen, B. S. Huang, Y. H. Yeh, and P. Shen (2005). Three-dimensional V_p and V_s structural models associated with the active subduction and collision tectonics in the Taiwan region from 3-D seismic tomography, *Geophys. J. Int.* (in press).
- Kissling, E., W. L. Ellsworth, D. Eberhart-Phillips, and U. Kradolfer (1994). Initial reference models in local earthquake tomography, *J. Geophys. Res.* **99**, no. B10, 19,635–19,646.
- Lee, C. R., and W. T. Cheng (1986). Preliminary heat flow measurements in Taiwan, Presented at the Fourth Circum-Pacific Energy and Mineral Resources Conference, Singapore.
- Lee, C. T. (1999). Neotectonics and Active Fault in Taiwan, Presented at the Workshop on Disaster Prevention/Management and Green Technology, Foster City, California, 61–74.
- Liang, W. T., and J. M. Chiu (2006). Anomalous P_n waves observed in eastern Taiwan: implications of an elevated upper mantle beneath the active collision suture zone, *Geophys. Res. Lett.* (in press).
- Lin, C. H., Y. H. Yeh, H. Y. Yen, K. C. Chen, B. S. Huang, S. Roecker, and J. M. Chiu (1998). Three-dimensional elastic wave velocity structure of the Hualien region of Taiwan: evidence of active crustal exhumation, *Tectonics* **17**, no. 1, 89–103.
- Ma, K. F., J. H. Wang, and D. Zhao (1996). Three-dimensional seismic velocity structure of the crust and uppermost mantle beneath Taiwan, *J. Phys. Earth* **44**, no. 2, 85–105.
- Okubo, P. G., H. M. Benz, and B. A. Chouet (1997). Imaging the crustal magma sources beneath Mauna Loa and Kilauea volcanoes, Hawaii, *Geology* **25**, no. 10, 867–870.
- Podvin, P., and I. Lecomte (1991). Finite difference computation of traveltimes in very contrasted velocity models; a massively parallel approach and its associated tools, *Geophys. J. Int.* **105**, no. 1, 271–284.
- Shen, P. (1999). Simultaneous travel time inversion for 3-D velocity model and earthquake locations: Application to the Northridge, California, 1994 mainshock-aftershock sequence. *Master's Thesis*, The University of Memphis, Memphis, 117 pp.
- Snoke, A. J., and J. C. Lahr (2001). Locating earthquakes: at what distances can the earth no longer be treated as flat? *Seism. Res. Lett.* **72**, no. 5, 538–541.
- Tsai, Y. B. (1986). Seismotectonics of Taiwan, *Tectonophysics* **125**, 17–37.
- Villasenor, A., R. Scarpa, G. Patane, S. Vinciguerra, H. M. Benz, L. Filippi, and G. De Luca (1998). Three-dimensional P-wave velocity structure of Mt. Etna, Italy, *Geophys. Res. Lett.* **25**, no. 11, 1975–1978.
- Waldausser, F., and W. L. Ellsworth (2000). A double-difference earthquake location algorithm: method and application to the northern Hayward fault, California, *Bull. Seism. Soc. Am.* **90**, no. 6, 1353–1368.
- Wang, J. H., K. C. Chen, and T. Q. Lee (1994). Depth distribution of shallow earthquakes in Taiwan, *J. Geol. Soc. China* **37**, no. 2, 125–142.
- Wessel, P., and W. H. F. Smith (1991). Free software helps map and display data, *EOS* **72**, 441, 445–446.
- Wessel, P., and W. H. F. Smith (1995). New version of the Generic Mapping Tools released, *EOS* **76**, 329.
- Yeh, Y. H., H. Y. Yen, K. C. Chen, J. M. Chiu, C. H. Lin, W. T. Liang, B. S. Huang, C. R. Lin, and T. Y. Hou (1997). A high-resolution seismic array experiment in the Hualien area, Taiwan, *TAO* **8**, no. 3, 329–344.
- Yu, S. B., and L. C. Kuo (2001). Present-day crustal motion along the Longitudinal Valley fault, eastern Taiwan, *Tectonophysics* **333**, no. 1–2, 199–217.
- Yu, S. B., and C. C. Liu (1989). Fault creep on the central segment of the Longitudinal Valley Fault, eastern Taiwan, *Proc. Geol. Soc. China* **32**, no. 3, 209–231.
- Yu, S. B., H. Y. Chen, L. C. Kuo, S. E. Lallemand, and H. H. Tsien (1997). Velocity field of GPS stations in the Taiwan area, *Tectonophysics* **274**, no. 1–3, 41–59.
- Yu, S. B., D. D. Jackson, G. K. Yu, and C. C. Lin (1990). Dislocation model for crustal deformation in the Longitudinal Valley area, eastern Taiwan, *Tectonophysics* **183**, no. 1–4, 97–109.
- Zhao, D., A. Hasegawa, and S. Horiuchi (1992). Tomographic imaging of P and S wave velocity structure beneath northeastern Japan, *J. Geophys. Res.* **97**, no. 13, 19,909–19,928.

Institute of Earth Sciences
Academia Sinica
P.O. Box 1-55
Nankang, Taipei, 11529 Taiwan
(K.H.K., K.-C.C.)

Center for Earthquake Research and Information
The University of Memphis
Memphis, Tennessee 38152
(K.H.K., J.M.C.)

Department of Earth Sciences
The University of Memphis
Memphis, Tennessee 38152
(J.P.)

Manuscript received 26 May 2005.